Journal of Applied Analysis and Computation
Volume 13, Number 5, October 2023, 2682–2702
Website:http://www.jaac-online.com
DOI:10.11948/20220534

HOPF BIFURCATION AND CHAOS OF COMBINATIONAL IMMUNE ANTI-TUMOR MODEL WITH DOUBLE DELAYS*

Jingnan Wang[1,†], Lu Zang[1] and Li Xu[1]

Abstract In order to investigate the relations between tumor species growth and T cell activation assisted by dendritic cells, we establish a combinational immune anti-tumor model with double delays. Taking the activation rate of T cell and two time delays of tumor species growth and dendritic cell activation as parameters, we investigate the dynamical properties of the double delayed model, including the stability switches and the Hopf bifurcations of tumor-escape equilibrium and tumor-present equilibrium. With Hopf bifurcation curves, the center manifold theory and the normal form method, we find bi-stability states, the coexistence of two periodic solutions with different stabilities, two double Hopf bifurcation points, and use numerical simulations to show rich dynamic behaviors around the double Hopf bifurcation points, including the phase portraits and the corresponding Poincaré maps of chaotic attractors, as well as the progress transmission of unstable-oscillation-stable-oscillation. The theoretical and numerical results reveal the new methods of controlling tumor cells.

Keywords Tumor-immune model, double time delays, chaotic attractor, stability switch, Hopf bifurcation.

MSC(2010) 34A36, 34C25.

1. Introduction

With the advent of the 5G era, many biomathematicians have used tumor-immune models to investigate the dynamic behaviors of tumor cells and immune cells, and to explore the laws in the tumor cell growth and T cell activation [7–9, 14, 15, 19, 27], which can provide some theoretical support for the developing effective strategies of tumor immunotherapy.

Tumor-immune models with time delays and dynamical behaviors induced by time delays have been widely investigated [2, 16, 25]. Many mathematical models show that time delays induce various possible bifurcations including Hopf,Hopf-zero and double Hopf bifurcations [3, 23, 24, 26]. According to the normal form method and the center manifold theory, the stability and direction of the Hopf bifurcation

†The corresponding author.
1Department of applied mathematics, Harbin University of Science and technology, Harbin, 150080, China
*The authors are supported by National Natural Science Foundation of China (11801122).
Email: wangjingnan@hrbust.edu.cn(J. Wang), zl353792@163.com(L. Zang), xuli_0220@163.com(L. Xu)

in models are determined [13, 20, 21]. Besides, it is found that the multiple delays can lead the system dynamic behavior to exhibit stability switches [1,22]. Using the crossing curve methods, the stable changes of equilibrium in two-delay parameter plane can be obtained [6, 10, 29]. Lin and Wang [11] use an algebraic method to derive a closed form for stability switching curves of delayed systems with two delays and delay independent coefficients. Therefore, we introduce two time delays of tumor species growth and dendritic cell activation into the model of Nagata and Furuta et al [14]. The specific is as follows

$$\begin{cases} \dfrac{\mathrm{d}C_H(t)}{\mathrm{d}t} = rC_H(t)\left(1 - \dfrac{C_H(t-\tau_1)}{K}\right) - cC_H(t)N_T(t), \\ \dfrac{\mathrm{d}N_T(t)}{\mathrm{d}t} = bN_T(t)N_{DC}(t) - \delta N_T(t), \\ \dfrac{\mathrm{d}N_{DC}(t)}{\mathrm{d}t} = aC_H(t-\tau_2)N_T(t-\tau_2) - \beta N_{DC}(t), \end{cases} \tag{1.1}$$

where $C_H(t)$, $N_T(t)$, $N_{DC}(t)$ denote the densities of tumor cells, activated T cells and activated dendritic cells, respectively. r is the tumor population growth rate and K is the carrying capacity. a and b represent the activation rates of dendritic cells and T cells, respectively. δ and β represent the inactivation rates of T cells and dendritic cells, respectively. c is the tumor killing rate by T cells. τ_1 is the feedback time delay of tumor cells to the species itself growth, and τ_2 is the time delay of the dendritic cell activation during antigen presentation. In model (1.1) with $\tau_1 = \tau_2 = 0$ in [14], $E_0(0, 0, 0)$ is an unstable equilibrium and $E_K(K, 0, 0)$ is a locally asymptotically stable equilibrium, $E_+^*(C_H^+, N_T^+, \frac{\delta}{b})$ is an unstable tumor-present equilibrium when $\rho_0 > 1$, $E_-^*(C_H^-, N_T^-, \frac{\delta}{b})$ is a locally asymptotically stable tumor-present equilibrium when $\rho_0 > 1$ and if and only if

$$-\frac{abr^2}{2c} - \frac{abr\beta}{2c} + \frac{r\delta\beta}{K} + \frac{r^2\beta}{2K} + \frac{r\beta^2}{K} - \frac{r\sqrt{1-1/\rho_0}}{2}\left(\frac{r\beta}{K} + \frac{ab\beta}{c} + \frac{abr}{c}\right) > 0, \tag{1.2}$$

where

$$C_H^{\pm} = \frac{K}{2}\left(1 \pm \sqrt{1 - \frac{1}{\rho_0}}\right),\ N_T^{\pm} = \frac{r}{2c}\left(1 \mp \sqrt{1 - \frac{1}{\rho_0}}\right),\ \rho_0 = \frac{abrK}{4c\delta\beta}. \tag{1.3}$$

For the convenience of discussion, we apply the following notation in model (1.1)

$$x(t) = C_H(t), y(t) = N_T(t), z(t) = N_{DC}(t), x_{\pm}^* = C_H^{\pm},\ y_{\pm}^* = N_T^{\pm}, z^* = \frac{\delta}{b}. \tag{1.4}$$

Then model (1.1) becomes the following form

$$\begin{cases} \dfrac{\mathrm{d}x(t)}{\mathrm{d}t} = rx(t)(1 - \dfrac{x(t-\tau_1)}{K}) - cx(t)y(t), \\ \dfrac{\mathrm{d}y(t)}{\mathrm{d}t} = by(t)z(t) - \delta y(t), \\ \dfrac{\mathrm{d}z(t)}{\mathrm{d}t} = ax(t-\tau_2)y(t-\tau_2) - \beta z(t). \end{cases} \tag{1.5}$$

The rest of the paper is organized as follows. In Sect. 2, we use the dendritic cell activation rate and time delays as parameters to determine the stability regions of tumor-present equilibrium and Hopf bifurcation properties of model (1.5) through the normal form theory. In Sect. 3, we use the Hopf bifurcation curve to find two double Hopf bifurcation points, and use numerical simulations to show rich dynamic behaviors around the double Hopf bifurcation points, including the interesting phase plane and the corresponding Poincaré map of chaotic attractors, as well as the progress transmission of unstable-oscillation-stable-oscillation. New methods of controlling tumor cells and concluding remarks are given in Sect.4.

2. Local stability and Hopf bifurcation properties

By referring to stability condition (1.2) in model (1.1) at equilibrium E_-^*, we obtain the following critical values of parameter b satisfying the stability condition of equilibrium E_-^* when $\tau_1 = \tau_2 = 0$.

Theorem 2.1. *Suppose $\tau_1 = \tau_2 = 0$. If $b_1^* < b < b_2^*$, then E_-^* of model (1.5) is locally asymptotically stable, where $b_1^* = \frac{4c\delta\beta}{arK}$, $b_2^* = \frac{c\beta\left(2(\delta+\beta)+r-r\sqrt{1-1/\rho_0}\right)}{aK(r+\beta)\left(1+\sqrt{1-1/\rho_0}\right)}$, ρ_0 is defined in equation* (1.3).

Proof. By the existence condition $\rho_0 = \frac{abrK}{4c\delta\beta} > 1$ of E_-^* in model (1.1), we obtain

$$b > \frac{4c\delta\beta}{arK} \doteq b_1^*.$$

By the stability condition (1.2) of E_-^* in model (1.1), we obtain

$$b < \frac{c\beta\left(2(\delta+\beta)+r-r\sqrt{1-1/\rho_0}\right)}{aK(r+\beta)\left(1+\sqrt{1-1/\rho_0}\right)} \doteq b_2^*.$$

Therefore, if $\tau_1 = \tau_2 = 0$ and $b_1^* < b < b_2^*$, then equilibrium E_-^* of model (1.5) is locally asymptotically stable. The proof of the theorem is completed. $\square$

The linearization characteristic equation of model (1.5) at the equilibrium $E_*(x_*, y_*, z_*)$ is

$$\det\begin{pmatrix} \lambda - r(1-\frac{x_*}{K}) + cy_* + \frac{rx_*}{K}e^{-\lambda\tau_1} & cx_* & 0 \\ 0 & \lambda+\delta-bz_* & -by_* \\ -ay_*e^{-\lambda\tau_2} & -ax_*e^{-\lambda\tau_2} & \lambda+\beta \end{pmatrix} = 0. \tag{2.1}$$

Through the expression of Eg. (2.1), we obtain

Theorem 2.2. *If $\tau_1 < \tau_{1K_0}$, then equilibrium E_K of model (1.5) is locally asymptotically stable for any $\tau_2 \geq 0$; if $\tau_1 > \tau_{1K_0}$, then equilibrium E_K of model (1.5) is unstable for any $\tau_2 \geq 0$; if $\tau_1 = \tau_{1K_0}$, then model (1.5) undergoes a Hopf bifurcation at E_K, where $\tau_{1K_0} = \frac{\pi}{2r}$.*

Proof. At E_K, the characteristic equation (2.1) becomes

$$(\lambda + re^{-\lambda\tau_1})(\lambda+\delta)(\lambda+\beta) = 0. \tag{2.2}$$

All the roots of equation (2.2) have negative real parts for any $\tau_2 \geq 0$ when $\tau_1 = 0$. If $\tau_1 = \tau_{1K_j}$ (where $\tau_{1K_j} \doteq \frac{1}{r}[\frac{\pi}{2} + 2j\pi]$, $j = 0, 1, \cdots$), then equation (2.2) has a pair of purely imaginary roots $\lambda = \pm ir$, and

$$\frac{\mathrm{dRe}(\lambda)}{\mathrm{d}\tau_1}\bigg|_{\lambda=ir,\tau_1=\tau_{1K_0}=\frac{\pi}{2r}} = \frac{r^2}{1+(\frac{\pi}{2})^2} > 0.$$

By Corollary 2.3 in [17], we know that for any $\tau_2 \geq 0$, equilibrium E_K of model (1.5) is locally asymptotically stable when $\tau_1 < \tau_{1K_0}$ and it is unstable when $\tau_1 > \tau_{1K_0}$. In addition, model (1.5) undergoes a Hopf bifurcation at E_K when $\tau_1 = \tau_{1K_0}$. The proof of the theorem is completed. □

The characteristic equation(2.1) of E_-^* is

$$D(\lambda,\tau_1,\tau_2) = P_0(\lambda) + P_1(\lambda)e^{-\lambda\tau_1} + P_2(\lambda)e^{-\lambda\tau_2} + P_3(\lambda)e^{-\lambda(\tau_1+\tau_2)} = 0 \qquad (2.3)$$

where

$$\begin{aligned} &P_0(\lambda) = \lambda^3 + \beta\lambda^2, \quad P_1(\lambda) = \frac{rx_-^*}{K}\lambda^2 + \frac{\beta r x_-^*}{K}\lambda, \\ &P_2(\lambda) = \delta\beta(-\lambda + r(1-\frac{x_-^*}{K})), \quad P_3(\lambda) = -\frac{\delta\beta r x_-^*}{K}. \end{aligned} \qquad (2.4)$$

In order to study the stability of E_-^* when $\tau_1 > 0$ or $\tau_2 > 0$, we obtain that equation (2.3) has the purely imaginary roots under the following two cases:

Case(I): Fixed delay τ_1 and $\tau_2 > 0$.

Suppose that equation (2.3) has a purely imaginary root $\lambda = i\omega$, and substituting it into Eq. (2.3) we have

$$\Theta(\omega,\tau_1) = L(\omega,\tau_1)e^{-i\omega\tau_2} \qquad (2.5)$$

where

$$\Theta(\omega,\tau_1) = P_0(i\omega) + P_1(i\omega)e^{-i\omega\tau_1}, \; L(\omega,\tau_1) = -P_2(i\omega) - P_3(i\omega)e^{-i\omega\tau_1}. \qquad (2.6)$$

Separating the real and imaginary parts of Eq. (2.5), we have

$$\begin{cases} \cos(\omega\tau_2) = \dfrac{\mathrm{Re}\,[\Theta(\omega,\tau_1)]\,\mathrm{Re}\,[L(\omega,\tau_1)] + \mathrm{Im}\,[\Theta(\omega,\tau_1)]\,\mathrm{Im}\,[L(\omega,\tau_1)]}{\mathrm{Re}^2\,[L(\omega,\tau_1)] + \mathrm{Im}^2\,[L(\omega,\tau_1)]} \doteq M_{\tau_1 C}(\omega), \\ \sin(\omega\tau_2) = \dfrac{\mathrm{Re}\,[\Theta(\omega,\tau_1)]\,\mathrm{Im}\,[L(\omega,\tau_1)] - \mathrm{Im}\,[\Theta(\omega,\tau_1)]\,\mathrm{Re}\,[L(\omega,\tau_1)]}{\mathrm{Re}^2\,[L(\omega,\tau_1)] + \mathrm{Im}^2\,[L(\omega,\tau_1)]} \doteq M_{\tau_1 S}(\omega). \end{cases} \qquad (2.7)$$

Adding the squares of two equations of (2.7), we obtain

$$G_1(\omega,\tau_1) = \omega^6 + l_{11}\omega^5 + l_{12}\omega^4 + l_{13}\omega^3 + l_{14}\omega^2 + l_{15}\omega + l_{16} = 0. \qquad (2.8)$$

where

$$\begin{aligned} &l_{11} = -2\frac{rx_-^*}{K}\sin(\omega\tau_1), \quad l_{12} = \beta^2 + (\frac{rx_-^*}{K})^2, \quad l_{13} = -2\beta^2\frac{rx_-^*}{K}\sin(\omega\tau_1), \\ &l_{14} = \beta^2(\frac{rx_-^*}{K})^2 - \delta^2\beta^2, \quad l_{15} = 2\delta^2\beta^2\frac{rx_-^*}{K}\sin(\omega\tau_1), \\ &l_{16} = \delta^2\beta^2r^2[2\frac{x_-^*}{K}(1-\frac{x_-^*}{K}) - 1 + 2\frac{x_-^*}{K}(1-\frac{x_-^*}{K})\cos(\omega\tau_1)]. \end{aligned} \qquad (2.9)$$

If (2.8) has a number of positive and simple roots $\omega_{\tau_1}^k$ $(k = 1, 2, \cdots)$, then the characteristic equation (2.3) has a series of critical delays

$$\tau_{2_j}^k = \begin{cases} \dfrac{1}{\omega_{\tau_1}^k}[\arccos(M_{\tau_1 C}(\omega_{\tau_1}^k)) + 2j\pi], \quad M_{\tau_1 S}(\omega_{\tau_1}^k) \geq 0, \\ \dfrac{1}{\omega_{\tau_1}^k}[-\arccos(M_{\tau_1 C}(\omega_{\tau_1}^k)) + 2(j+1)\pi], \quad M_{\tau_1 S}(\omega_{\tau_1}^k) < 0. \end{cases} \qquad (2.10)$$

Clearly, when $\tau_1 = 0$, for $\beta^2 + (\frac{rx_-^*}{K})^2 > 0$ and $x_-^* < K/2$,

$$G_1(\omega^2, 0) =(\omega^2)^3 + \frac{\beta^2 K^2 + (rx_-^*)^2}{K^2}(\omega^2)^2 + \frac{\beta^2\left((rx_-^*)^2 - K^2\delta^2\right)}{K^2}\omega^2 - \frac{(\delta\beta r(K - 2x_-^*))^2}{K^2} = 0 \tag{2.11}$$

has a unique positive root ω_0. Thus equation (2.3) at $\tau_1 = 0$ has a series of critical delays

$$\tau_{2_j}^0 = \begin{cases} \frac{1}{\omega_0}\left[\arccos(\frac{-\delta\beta K^2\omega_0^4 + \left[\delta\beta r(K-2x_-^*)(K\beta + rx_-^*) + \delta\beta^2 K r x_-^*\right]\omega_0^2}{K^2\delta^2\beta^2\omega_0^2 + \delta^2\beta^2 r^2 (K-2x_-^*)^2}) + 2j\pi\right], & M_{0S}(\omega_0) \geq 0, \\ \frac{1}{\omega_0}\left[-\arccos(\frac{-\delta\beta K^2\omega_0^4 + \left[\delta\beta r(K-2x_-^*)(K\beta + rx_-^*) + \delta\beta^2 K r x_-^*\right]\omega_0^2}{K^2\delta^2\beta^2\omega_0^2 + \delta^2\beta^2 r^2 (K-2x_-^*)^2}) + 2(j+1)\pi\right], & M_{0S}(\omega_0) < 0, \end{cases}$$

where $M_{0S}(\omega_0) = \sin(\omega_0\tau_{2_j}^0) = \frac{\delta\beta K(rx_-^* - K\beta - Kr)\omega_0^3 + \delta\beta^2 r(K-2x_-^*)rx_-^*\omega_0}{K^2\delta^2\beta^2\omega_0^2 + \delta^2\beta^2 r^2(K-2x_-^*)^2}$.

Through routine calculation, we have

$$\begin{aligned} \mathrm{Sign}\left[\frac{\mathrm{dRe}(\lambda)}{\mathrm{d}\tau_2}\right]_{\lambda=i\omega_0,\tau_2=\tau_{2_j}^0} &= \mathrm{Sign}\left\{\mathrm{Re}\left[\frac{\mathrm{d}\lambda}{\mathrm{d}\tau_2}\right]^{-1}_{\lambda=i\omega_0,\tau_2=\tau_{2_j}^0}\right\} \\ &= \mathrm{Sign}\left\{\frac{\mathrm{d}G_1(\omega^2,0)}{\mathrm{d}\omega^2}|_{\omega^2=\omega_0^2}\right\}. \end{aligned}$$

Thus, we have

Lemma 2.1. *If* $\delta < \frac{1}{2}r(1 - \sqrt{1 - 1/\rho_0})$, *then* $\mathrm{Sign}\left[\frac{\mathrm{dRe}(\lambda)}{\mathrm{d}\tau_2}\right]_{\lambda=i\omega_0,\tau_2=\tau_{2_j}^0} > 0$.

By Lemma 2.1, we have

Theorem 2.3. *For* $\tau_1 = 0$. *Suppose that* $b_1^* < b < b_2^*$ *and* $\delta < \frac{1}{2}r(1 - \sqrt{1 - 1/\rho_0})$ *hold, then equilibrium* E_-^* *of model (1.5) is locally asymptotically stable for* $\tau_2 < \tau_{2_0}^0$ *and unstable for* $\tau_2 > \tau_{2_0}^0$. *Furthermore, model (1.5) undergoes a Hopf bifurcation at* E_-^* *when* $\tau_2 = \tau_{2_0}^0$, *where* b_1^* *and* b_2^* *are defined as in Theorem 2.1.*

Case(II): Fixed delay τ_2 and $\tau_1 > 0$.

Following a similar computing process for the fixed τ_1, we have

$$G_2(\omega, \tau_2) = \omega^6 + l_{21}\omega^5 + l_{22}\omega^4 + l_{23}\omega^3 + l_{24}\omega^2 + l_{25}\omega + l_{26} = 0. \tag{2.12}$$

where

$$l_{21} = 0,\ l_{22} = \beta^2 - (\frac{rx_-^*}{K})^2 + 2\delta\beta\cos(\omega\tau_2),\ l_{23} = 2\delta\beta[r(1 - \frac{x_-^*}{K}) + \beta]\sin(\omega\tau_2),$$

$$l_{24}=\delta^2\beta^2-(\beta\frac{rx_-^*}{K})^2-2\delta\beta[(\frac{rx_-^*}{K})^2+\beta r(1-\frac{x_-^*}{K})]\cos(\omega\tau_2),$$
$$l_{25}=-2\delta\beta^2(\frac{rx_-^*}{K})^2\sin(\omega\tau_2),\quad l_{26}=\delta^2\beta^2r^2(1-\frac{2x_-^*}{K}).$$

If (2.12) has a number of positive and simple roots $\omega_{\tau_2}^k$ $(k=1,2,\cdots)$, then equation (2.3) has a series of critical delays

$$\tau_{1_j}^k=\begin{cases}\frac{1}{\omega_{\tau_2}^k}\left[\arccos(\frac{\mathrm{Re}\big[\Theta(\omega_{\tau_2}^k,\tau_2)\big]\mathrm{Re}\big[L(\omega_{\tau_2}^k,\tau_2)\big]+\mathrm{Im}\big[\Theta(\omega_{\tau_2}^k,\tau_2)\big]\mathrm{Im}\big[L(\omega_{\tau_2}^k,\tau_2)\big]}{\mathrm{Re}^2\big[L(\omega_{\tau_2}^k,\tau_2)\big]+\mathrm{Im}^2\big[L(\omega_{\tau_2}^k,\tau_2)\big]})\right],\\ \quad M_{S\tau_2}(\omega_{\tau_2}^k)\geq 0,\\ \frac{1}{\omega_{\tau_2}^k}\left[-\arccos(\frac{\mathrm{Re}\big[\Theta(\omega_{\tau_2}^k,\tau_2)\big]\mathrm{Re}\big[L(\omega_{\tau_2}^k,\tau_2)\big]+\mathrm{Im}\big[\Theta(\omega_{\tau_2}^k,\tau_2)\big]\mathrm{Im}\big[L(\omega_{\tau_2}^k,\tau_2)\big]}{\mathrm{Re}^2\big[L(\omega_{\tau_2}^k,\tau_2)\big]+\mathrm{Im}^2\big[L(\omega_{\tau_2}^k,\tau_2)\big]})\right.\\ \quad\left.+2(j+1)\pi\right],\qquad M_{S\tau_2}(\omega_{\tau_2}^k)<0,\end{cases}\tag{2.13}$$

where

$$\begin{aligned}M_{S\tau_2}(\omega_{\tau_2}^k)&=\sin(\omega_{\tau_2}^k\tau_{1_j}^k)\\&=\frac{\mathrm{Re}\left[\Theta(\omega_{\tau_2}^k,\tau_2)\right]\mathrm{Im}\left[L(\omega_{\tau_2}^k,\tau_2)\right]-\mathrm{Im}\left[\Theta(\omega_{\tau_2}^k,\tau_2)\right]\mathrm{Re}\left[L(\omega_{\tau_2}^k,\tau_2)\right]}{\mathrm{Re}^2\left[L(\omega_{\tau_2}^k,\tau_2)\right]+\mathrm{Im}^2\left[L(\omega_{\tau_2}^k,\tau_2)\right]},\end{aligned}$$

where

$$\Theta(\omega_{\tau_2}^k,\tau_2)=P_0(i\omega_{\tau_2}^k)+P_2(i\omega_{\tau_2}^k)e^{-i\omega_{\tau_2}^k\tau_2},\ L(\omega_{\tau_2}^k,\tau_2)=-P_1(i\omega_{\tau_2}^k)-P_3(i\omega_{\tau_2}^k)e^{-i\omega_{\tau_2}^k\tau_2}.$$

When $\tau_2=0$, from Eq. (2.12), we obtain

$$\begin{aligned}G_2(\omega^2,0)=&(\omega^2)^3+\left[\beta^2+2\delta\beta-\left(\frac{rx_-^*}{K}\right)^2\right](\omega^2)^2+\left[\delta^2\beta^2-2\delta\beta^2r\left(1-\frac{x_-^*}{K}\right)\right.\\&\left.-(\beta^2+2\delta\beta)\left(\frac{rx_-^*}{K}\right)^2\right]\omega^2+\delta^2\beta^2r^2\left(1-\frac{2x_-^*}{K}\right)=0\end{aligned}\tag{2.14}$$

and

$$\begin{aligned}G_2'(\omega^2,0)=&3(\omega^2)^2+2\left[\beta^2+2\delta\beta-\left(\frac{rx_-^*}{K}\right)^2\right]\omega^2+\delta^2\beta^2-2\delta\beta^2r\left(1-\frac{x_-^*}{K}\right)\\&-(\beta^2+2\delta\beta)\left(\frac{rx_-^*}{K}\right)^2.\end{aligned}$$

Then the roots of $G_2'(\omega^2,0)=0$ can be expressed as

$$\omega_{01}^2=\frac{r^2(x_-^*)^2/K^2-\beta^2-2\delta\beta+\sqrt{\zeta}}{3},\quad \omega_{02}^2=\frac{r^2(x_-^*)^2/K^2-\beta^2-2\delta\beta-\sqrt{\zeta}}{3},$$

where

$$\zeta=\beta^4+\delta^2\beta^2+(\frac{rx_-^*}{K})^4+4\delta\beta^3+(2\delta\beta+\beta^2)(\frac{rx_-^*}{K})^2+6\delta\beta^2r(1-\frac{x_-^*}{K})>0.$$

According to Lemma 3.2 and Fig.a in [12], if the Hypothesis

$$(\mathbf{H}1) \quad \omega_{01}^2 > 0, \quad G_2(\omega_{01}^2, 0) < 0$$

holds, then Eq. (2.14) has two positive roots ω_-^2 and ω_+^2. Let $\omega_-^2 < \omega_+^2$, and then

$$G_2'(\omega_-^2, 0) < 0, G_2'(\omega_+^2, 0) > 0.$$

The corresponding series of critical delays are as follows

$$\tau_{1_j}^{\pm} = \begin{cases} \dfrac{1}{\omega_\pm}\left[\arccos(\dfrac{\delta\beta(K-x_-^*)\omega_\pm^2 + \delta^2\beta^2(K-x_-^*)}{x_-^*\omega_\pm^4 + (\beta^2+2\delta\beta)x_-^*\omega_\pm^2 + \delta^2\beta^2 x_-^*}) + 2j\pi\right], \quad M_{S0}(\omega_\pm) \geq 0, \\ \dfrac{1}{\omega_\pm}\left[-\arccos(\dfrac{\delta\beta(K-x_-^*)\omega_\pm^2 + \delta^2\beta^2(K-x_-^*)}{x_-^*\omega_\pm^4 + (\beta^2+2\delta\beta)x_-^*\omega_\pm^2 + \delta^2\beta^2 x_-^*}) + 2(j+1)\pi\right], \\ \quad M_{S0}(\omega_\pm) < 0, \end{cases}$$

$j = 0, 1, \cdots,$

where

$$M_{S0}(\omega_\pm) = \sin(\omega_\pm\tau_1) = \frac{K\omega_\pm^5 + (\beta^2+2\delta\beta)K\omega_\pm^3 + \delta\beta^2\left(\delta K - r\left(K - x_-^*\right)\right)\omega_\pm}{rx_-^*\omega_\pm^4 + r(\beta^2+2\delta\beta)x_-^*\omega_\pm^2 + \delta^2\beta^2 r x_-^*}.$$

Through routine calculation, we have

$$\begin{aligned} \mathrm{Sign}\left\{\left[\frac{\mathrm{dRe}(\lambda)}{\mathrm{d}\tau_1}\right]_{\lambda=i\omega_\pm, \tau_1=\tau_{1_j}^\pm}\right\} &= \mathrm{Sign}\left\{\mathrm{Re}\left[\frac{\mathrm{d}\lambda}{\mathrm{d}\tau_1}\right]^{-1}_{\lambda=i\omega_\pm, \tau_1=\tau_{1_j}^\pm}\right\} \\ &= \mathrm{Sign}\left\{\frac{\mathrm{d}G_2(\omega^2,0)}{\mathrm{d}\omega^2}|_{\omega^2=\omega_\pm^2}\right\}. \end{aligned}$$

From [13] and Corollary 2.4 in Ruan and Wei [18], we have the following conclusions about E_-^* when $\tau_2 = 0$.

Theorem 2.4. *For $\tau_2 = 0$, suppose $(\mathbf{H}1)$ holds. If $b_1^* < b < b_2^*$ and $\tau_{1_0}^+ < \tau_{1_0}^- < \tau_{1_1}^+$, then there is a positive integer m such that the equilibrium E_-^* of model (1.5) is stable when $\tau_1 \in [0, \tau_{1_0}^+) \cup (\tau_{1_0}^-, \tau_{1_1}^+) \cup \cdots \cup (\tau_{1_{m-1}}^-, \tau_{1_m}^+)$ and unstable when $\tau_1 \in [\tau_{1_0}^+, \tau_{1_0}^-) \cup (\tau_{1_1}^+, \tau_{1_1}^-) \cup \cdots \cup (\tau_{1_m}^+, \infty)$; if $b_1^* < b < b_2^*$, $\tau_{1_1}^+ < \tau_{1_0}^-$, then the equilibrium E_-^* of model (1.5) is stable when $\tau_1 \in [0, \tau_{1_0}^+)$ and unstable when $\tau_1 \in [\tau_{1_0}^+, \infty)$; if $b_1^* < b$, $b > b_2^*$ and $\tau_{1_0}^- < \tau_{1_0}^+$, then there exists a positive integer m such that the equilibrium E_-^* of model (1.5) is unstable when $\tau_1 \in [0, \tau_{1_0}^-) \cup (\tau_{1_0}^+, \tau_{1_1}^-) \cup \cdots \cup (\tau_{1_m}^+, \infty)$ and stable when $\tau_1 \in [\tau_{1_0}^-, \tau_{1_0}^+) \cup (\tau_{1_1}^-, \tau_{1_1}^+) \cup \cdots\cdots \cup (\tau_{1_m}^-, \tau_{1_m}^+)$. Furthermore, model (1.5) undergoes a Hopf bifurcation at E_-^* when $\tau_1 = \tau_{1_j}^\pm$, $j = 0, 1, 2, \cdots$, where b_1^* and b_2^* are defined as in Theorem 2.1.*

In order to investigate the Hopf bifurcation condition of equilibrium E_-^* when $\tau_1 > 0$ and $\tau_2 > 0$, we deduce

$$\frac{\mathrm{d}\lambda}{\mathrm{d}\tau_m} = \frac{[P_m(\lambda)+P_3(\lambda)e^{-\lambda\tau_n}]\lambda e^{-\lambda\tau_m}}{P_0'(\lambda)+[P_1'(\lambda)-\tau_1 P_1(\lambda)]e^{-\lambda\tau_1}+[P_2'(\lambda)-\tau_2 P_2(\lambda)]e^{-\lambda\tau_2}-(\tau_1+\tau_2)P_3(\lambda)e^{-\lambda(\tau_1+\tau_2)}},$$

where $(m, n) = (1, 2)$ or $(m, n) = (2, 1)$.

In addition, we assume that

$$(\mathbf{H}2)\quad \mathrm{Sign}\left\{\left[\frac{\mathrm{dRe}(\lambda)}{\mathrm{d}\tau_1}\right]_{\lambda=i\omega^k_{\tau_2},\tau_1=\tau_1^*}\right\}\neq 0,$$

$$(\mathbf{H}3)\quad \mathrm{Sign}\left\{\left[\frac{\mathrm{dRe}(\lambda)}{\mathrm{d}\tau_2}\right]_{\lambda=i\omega^k_{\tau_1},\tau_2=\tau_2^*}\right\}\neq 0,$$

where $\tau_1^*=\min\{\tau^k_{1_j}|k=1,2,\cdots;j=0,1,2,\cdots\}$, $\tau_2^*=\min\{\tau^k_{2_j}|k=1,2,\cdots;j=0,1,2,\cdots\}$. $\omega^k_{\tau_1}$ and $\omega^k_{\tau_2}$ are the fixed solutions of equation (2.8) and equation (2.12), respectively. $\tau^j_{1_k}$ and $\tau^j_{2_k}$ are defined in equation (2.13) and equation (2.10), respectively.

Therefore, by the general Hopf bifurcation theorem for FDEs [4], we have the following results of stability and bifurcation in system (1.5).

Theorem 2.5. *If $\tau_2\in[0,\tau^0_{2_0})$, $b_1^*<b<b_2^*$ and $(\mathbf{H}2)$ holds, then the equilibrium E_-^* of model (1.5) is asymptotically stable when $\tau_1\in(0,\tau_1^*)$, and model (1.5) undergoes a Hopf bifurcation at E_-^* when $\tau_1=\tau_1^*$, where b_1^* and b_2^* are defined as in Theorem 2.1.*

Theorem 2.6. *If $\tau_1\in[0,\tau^+_{1_0})$, $b_1^*<b<b_2^*$, $(\mathbf{H}1)$ and $(\mathbf{H}3)$ hold, then the equilibrium E_-^* of model (1.5) is asymptotically stable when $\tau_2\in(0,\tau_2^*)$, and model (1.5) undergoes a Hopf bifurcation at E_-^* when $\tau_2=\tau_2^*$, where b_1^* and b_2^* are defined as in Theorem 2.1.*

By using the center manifold theory and the normal form method in Hassard et al [5], we obtain the detailed bifurcation properties at E_-^* of model (1.5) when $\tau_2=\tau_2^*$ and $\tau_1\in[0,\tau^+_{1_0})$ (or $\tau_1=\tau_1^*$ and $\tau_2\in[0,\tau^0_{2_0})$) through the following quantities (the computing process is in the Appendix):

$$\begin{aligned}
&C_1(0)=\frac{i}{2\omega^k_{\tau_n}\tau^*_m}\left(g_{20}g_{11}-2|g_{11}|^2-\frac{|g_{02}|^2}{3}\right)+\frac{g_{21}}{2},\\
&\mu_2=-\frac{\mathrm{Re}(C_1(0))}{\mathrm{Re}(\lambda'(\tau^*_m))},\\
&\beta_2=2\mathrm{Re}(C_1(0)),
\end{aligned}\tag{2.15}$$

where $(m,n)=(1,2)$ or $(m,n)=(2,1)$.

Theorem 2.7. *Suppose that the conditions of Theorem 2.5 (or Theorem 2.6) hold. Then μ_2 in Eq. (2.15) determines the direction of Hopf bifurcation. If $\mu_2>0$ ($\mu_2<0$), then Hopf bifurcation is forward (backward), and the bifurcation periodic orbits of model (1.5) at the tumor present equilibrium E_-^* exist for $\tau_l>\tau_l^*$ ($\tau_l<\tau_l^*$), $l=1,2$. β_2 in Eq. (2.15) determines the stability of the bifurcating periodic orbits. The bifurcating periodic orbits are asymptotically stable (unstable) if $\beta_2<0$ ($\beta_2>0$).*

3. Numerical simulations

Based on the results of linear stability analysis and bifurcation analysis in Section 2, and by referring the coefficients in [14], we choose the following coefficients of model(1.5)

$$K = 200,\ a = 0.02,\ b = 0.2,\ c = 1.2,\ r = 5.9453433,\ \beta = 1,\ \delta = 0.92. \tag{3.1}$$

Then we obtain the boundary equilibrium $E_K = (200, 0, 0)$, the coexistence equilibrium $E_+^* = (126.7474, 1.8146, 4.6)$ and $E_-^* = (73.2526, 3.1398, 4.6)$. By Theorem 2.1 and Theorem 2.2, we obtain that $b_1^* = 0.1857$, $b_2^* = 0.2793$ and $\tau_{1K_0} = 0.2642$. When $\tau_1 = \tau_2 = 0$ and $b = 0.2 \in (b_2^*, b_2^*)$, E_K and E_-^* are both locally asymptotically stable. Through routine calculation of Eq. (2.15), we obtain Hopf bifurcation values in Table 1 and Table 2.

Table 1. Hopf bifurcation points and some related values for different τ_1 and parameter condition (3.1)

τ_1	0	0.2
$\tau_{2_0}^0(\tau_{2_0}^k)$	0.688984	1.139005
$\omega_0(\omega_{\tau_1}^k)$	0.594730	0.593135
$\mathrm{Re}(C_1(0))$	−0.221747	−0.483950
$\mathrm{Re}\{\lambda'(\tau_2)\}$	0.121798	0.117847
μ_2	1.820604	4.106615
β_2	−0.443493	−0.967901

Table 2. The Hopf bifurcation values of fixed $\tau_2 = 0$ with parameter condition (3.1)

ω	$\omega_+ \approx 2.303010$		$\omega_- \approx 0.630177$	
$\tau_{1_j}^{\pm}$	$\tau_{1_0}^+ \approx 0.583536$	$\tau_{1_1}^+ \approx 3.311786$	$\tau_{1_0}^- \approx 9.681465$	$\tau_{1_1}^- \approx 19.651966$
$\mathrm{Re}(C_1(0))$	3.286613	0.786925	0.887951	0.867306
$\mathrm{Re}\{\lambda'(\tau_{1_j}^{\pm})\}$	3.312543	0.119292	−0.009410	−0.002195
μ_2	−0.992172	−6.596634	94.365686	395.098458
β_2	6.573226	1.573852	1.775902	1.734611

From Table 1, we know that when $\tau_1 = 0$, the Hopf bifurcation values of model (1.5) are

$$\tau_{2_0}^0 \approx 0.688984, \omega_0 \approx 0.594730, \left.\frac{\mathrm{dRe}(\lambda)}{\mathrm{d}\tau_2}\right|_{\lambda=0.594730i, \tau_1=0, \tau_2=0.688984} \approx 0.121798 > 0.$$

When $\tau_1 = 0$ and $\tau_2 = 0.3 < \tau_{2_0}^0$, the coexistence equilibrium E_-^* of model (1.5) is locally asymptotically stable (see the red line in Fig. 1). In addition, $\mu_2 \approx 1.820604 > 0$, $\beta_2 \approx -0.443493 < 0$ when $\tau_2 = \tau_{2_0}^0$, which means that when $\tau_2 > \tau_{2_0}^0$, there is a stable periodic solution bifurcating from E_-^* (see the green line in Fig. 1). The results of numerical simulations agree with the results of Theorem 2.3 and Theorem 2.7. In addition, with the increase of time delay τ_2, the amplitudes of the limit cycle increase (see the blue line in Fig. 1). From Fig. 1, E_K is always locally asymptotically stable with the increase of time delay τ_2 for $\tau_1 = 0$ (see Fig. 1).

From Table 2, we know that when $\tau_2 = 0$, the Hopf bifurcation values of model (1.5) are

$$\tau_{1_0}^+ \approx 0.583536, \omega_+ \approx 2.303010, \left.\frac{\mathrm{dRe}(\lambda)}{\mathrm{d}\tau_1}\right|_{\lambda=2.30301i, \tau_2=0, \tau_1=0.583536} \approx 3.3 > 0.$$

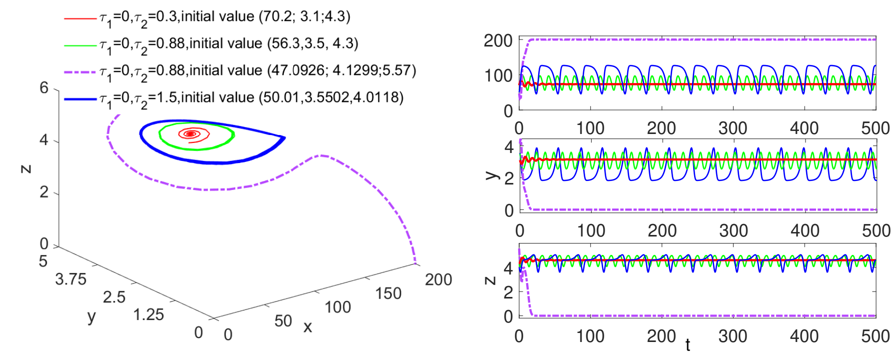

Figure 1. The phase plane and solution curves of model (1.5) with $\tau_1 = 0$.

When $\tau_2 = 0$ and $\tau_1 = 0.2(< \tau_{1K_0} < \tau_{1_0}^+)$, E_-^* and E_K of model (1.5) are both locally asymptotically stable simultaneously (see Fig. 2). In addition, since $\mu_2 \approx -0.99 < 0$ and $\beta_2 \approx 6.57 > 0$ when $\tau_1 = \tau_{1_0}^+$, model (1.5) undergoes two Hopf bifurcations at E_-^* and E_K, which means that when $\tau_2 = 0$ and $\tau_1 = 0.55 \in (\tau_{1K_0}, \tau_{1_0}^+)$, model (1.5) bifurcates an unstable periodic solution from E_-^*, and a stable periodic solution from E_K (see Fig. 3), respectively. The results of numerical simulations agree with the results of Theorem 2.2, Theorem 2.4, and Theorem 2.7.

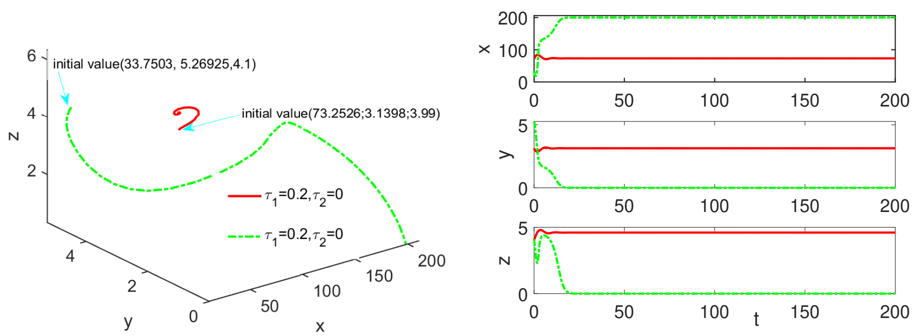

Figure 2. The phase plane and solution curves of model (1.5) with $\tau_1 = 0.2, \tau_2 = 0$.

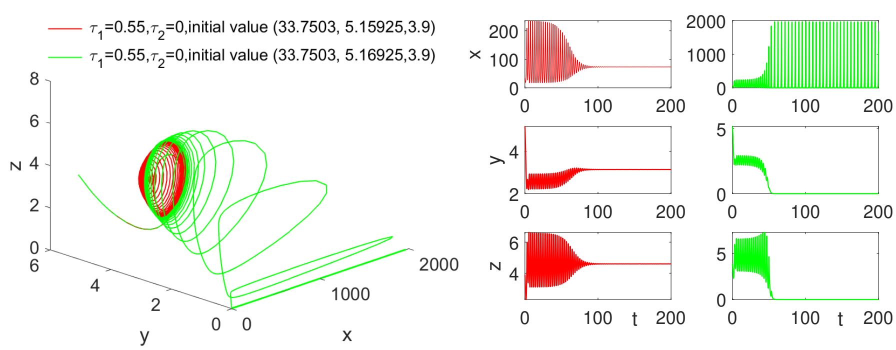

Figure 3. An unstable periodic oscillation and a stable periodic oscillation of model (1.5).

Besides, when fixed $\tau_1 = 0.2 \in [0, \tau_{1_0}^+)$, the Hopf bifurcation values of model (1.5) are

$$\tau_2^* \approx 1.139005, \omega_0 \approx 0.593135, \left.\frac{\mathrm{dRe}(\lambda)}{\mathrm{d}\tau_2}\right|_{\lambda=0.593135i,\tau_1=0.2,\tau_2=1.139005} \approx 0.117847 > 0.$$

When $\tau_1 = 0.2$ and $\tau_2 = 1 < \tau_2^*$, the coexistence equilibrium E_-^* is locally asymptotically stable (see red line in Fig. 4). In addition, since $\mu_2 \approx 4.106615 > 0$, $\beta_2 \approx -0.967901 < 0$, which means that when fixed $\tau_1 = 0.2$ and $\tau_2 = 1.3 > \tau_2^*$, there is a stable periodic solution bifurcating from E_-^* of model (1.5) (see green line in Fig. 4). The results of numerical simulations agree with the results of Theorem 2.6 and Theorem 2.7. In addition, when $\tau_2 = 2.3 > \tau_2^*$, E_K is still locally asymptotically stable for $\tau_1 = 0.2 < \tau_{1K_0} = 0.264206$ (see blue line in Fig. 4), numerical simulations agree with the results of Theorem 2.2.

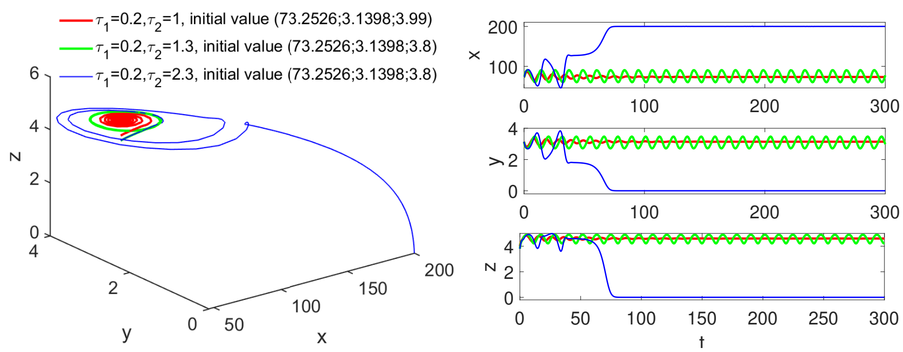

Figure 4. The phase plane and solution curves of model (1.5) with $\tau_1 = 0.2$.

We follow the process given in Section 2 of [11]. We obtain the stability switching curves $\mathcal{T}$ corresponding to $\Omega = [0.591335, 2.646868]$ (see the left of Fig. 5).

For a better understanding, we enlarge some area in the left of Fig. 5 and redraw them in the right of Fig. 5. From Fig. 5, the critical values agree with the critical values in Table 1 and Table 2.

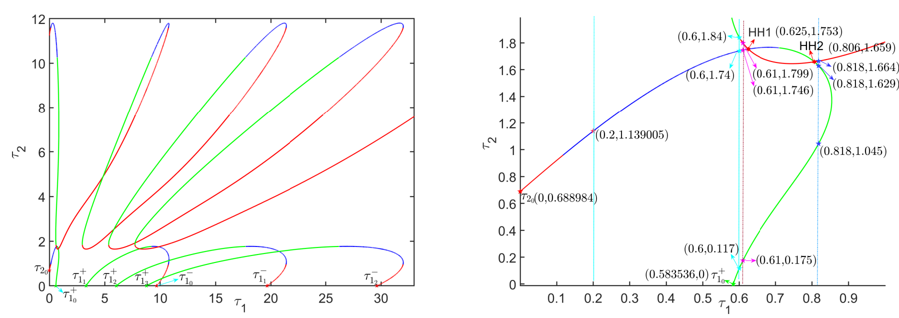

Figure 5. The stability switch curves on τ_1-τ_2 plane with coefficient condition (3.1).

Based on the stability switch curves of τ_1-τ_2 plane on the right of Fig. 5, we find double Hopf bifurcation points on the switch curves in Fig. 5, which means that

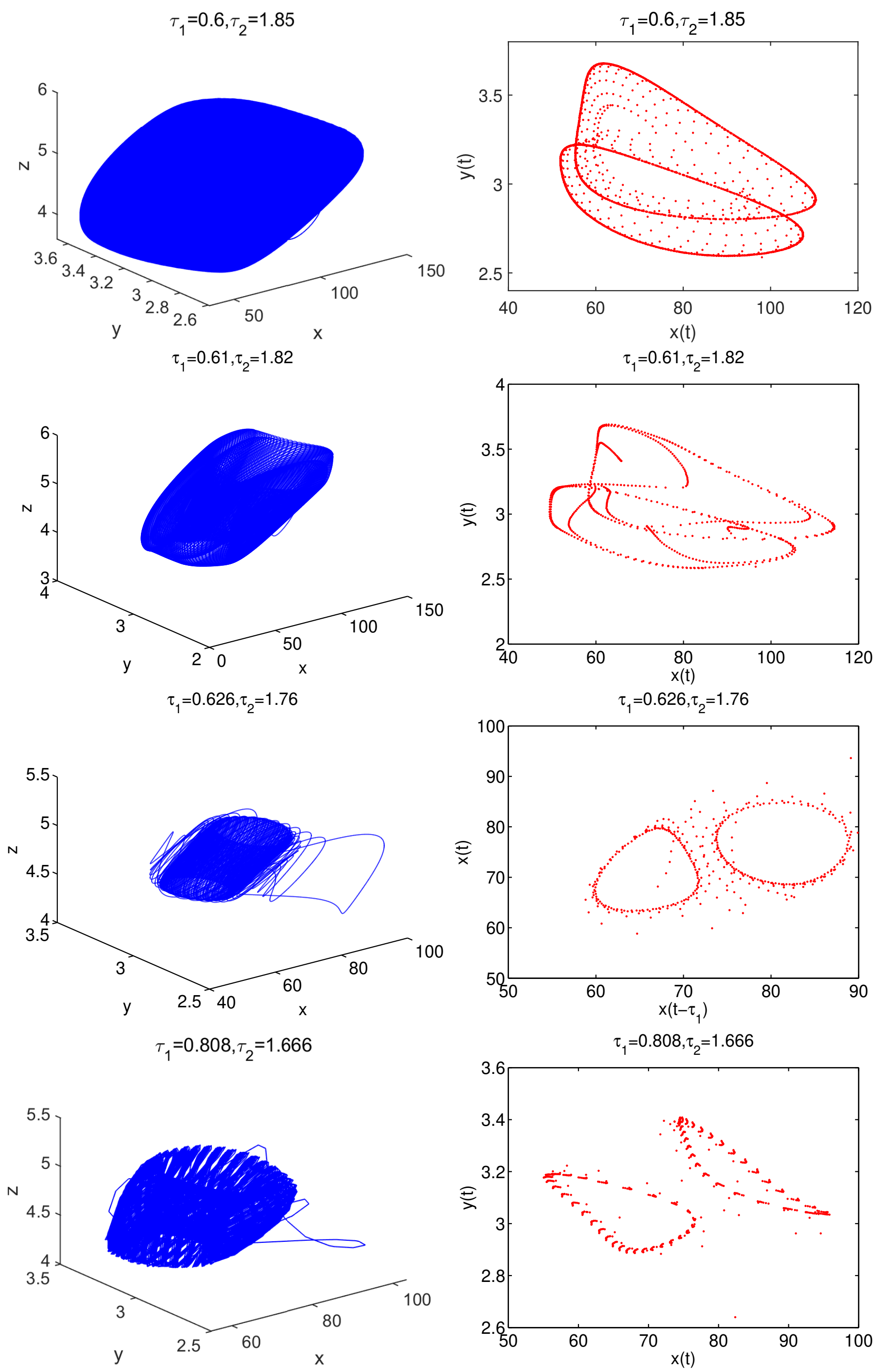

Figure 6. The phase portraits of chaotic attractors of model (1.5), and the corresponding Poincaré map on a Poincaré section $z(t) = z*$ with coefficient condition (3.1)

equation (2.3) has two pairs of purely imaginary eigenvalues simultaneously (see table 3).

Table 3. Values of double Hopf bifurcation Points

(τ_1, τ_2)	ω_1	ω_2	$\omega_1 : \omega_2$
$(0.624867, 1.753328)$	0.685504	2.634075	$\sqrt{7} : 10$
$(0.806451, 1.658745)$	0.854811	2.322703	$\sqrt{5} : 6$

If we choose $\tau_1 = 0.6$, $\tau_1 = 0.61$ or $\tau_1 = 0.818$ around the critical points of the double Hopf bifurcation, then we obtain three different critical values of τ_2^* corresponding to three different values of ω through calculation (see Fig. 5), that is to say, if τ_2 is greater than three critical values τ_2^*, then there exist three Hopf bifurcating periodic solutions with three amplitudes from Table 4. In addition, around the two double bifurcation points, the existence of several bifurcating periodic solutions can lead to chaotic attractors shaped like a bucket and a mushroom, as well as a solution shaped like a flower (their phase planes and the corresponding Poincaré maps see Figs. 6–8), respectively.

Table 4. The Hopf bifurcation values of fixed $\tau_1 = 0.6$, $\tau_1 = 0.61$ and $\tau_1 = 0.818$

τ_1		0.6			0.61			0.818	
$\tau_{2_0}^k$	0.117	1.74	1.84	0.175	1.746	1.799	1.045	1.629	1.664
$\omega_{\tau_1}^k$	2.188	0.67	2.65	2.130	0.678	2.645	1.334	0.879	2.302

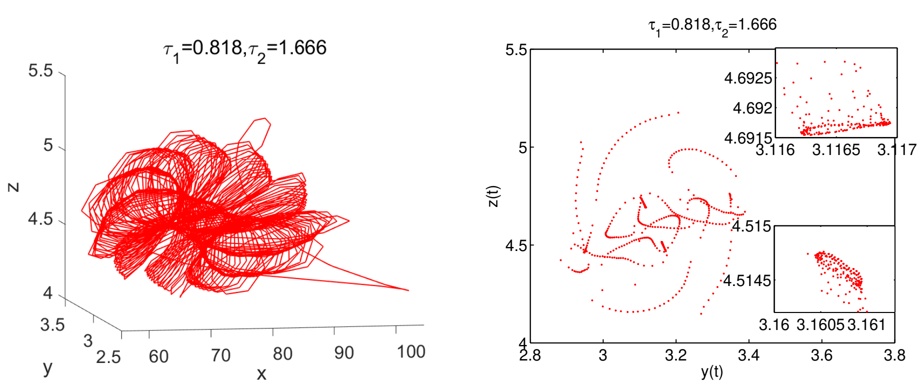

Figure 7. The phase portraits of chaotic attractors of model (1.5), and the corresponding Poincaré map on a Poincaré section $x(t) = x*$ with coefficient condition (3.1)

If we choose $b = 0.25$ and the other coefficients of mdel (1.5) do not change, we obtain that $b_1^* \approx 0.1857$ and $b_2^* \approx 0.194$. Since $\tau_1 = \tau_2 = 0$ and $b > b_2^*$, we know that $E_+^* = (150.7182, 1.2208, 3.68)$ and $E_-^* = (49.2818, 3.7336, 3.68)$ are both unstable by Theorem 2.1 and E_K is stable by Theorem 2.2 (see Fig. 10). Applying the same method of [11] to get the part stability switching curves $\mathcal{T}$ corresponding to $\Omega = [1.056066, 2.235792]$ (see Fig. 9). From Fig. 9, the critical values agree with the critical values in Table 5.

From Table 5, we know that when $\tau_1 = 0.2 < \tau_{1_0}^-$ and $\tau_2 = 0$, there exists a periodic oscillation in model (1.5) bifurcating from equilibrium E_-^* for $\mu_2 < 0$; when $\tau_1 = 0.5(\in (\tau_{1_0}^-, \tau_{1_0}^+))$ and $\tau_2 = 0$, E_-^* of model (1.5) becomes locally asymptotically

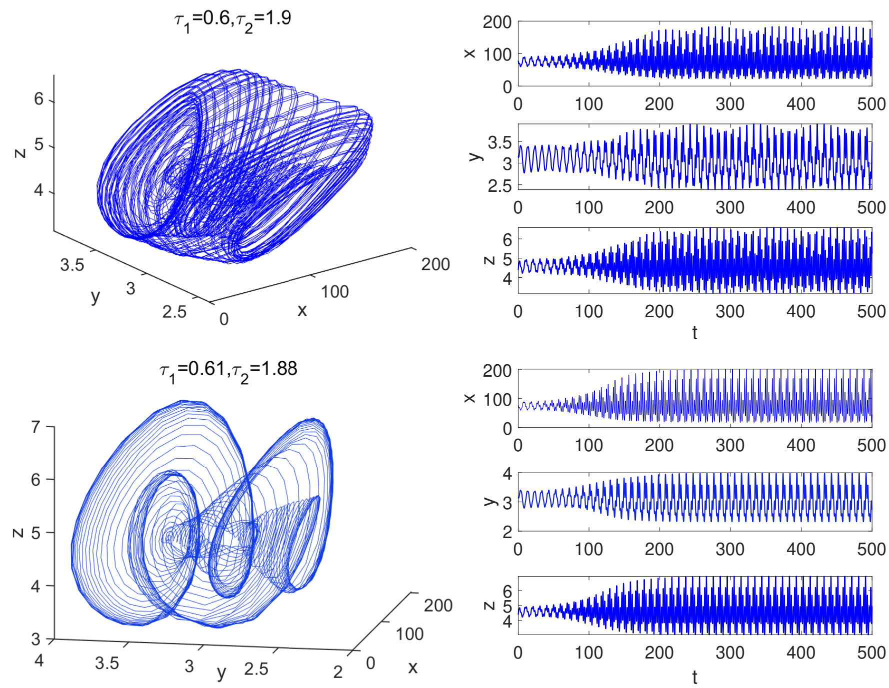

Figure 8. Chaotic attractors of model (1.5) with coefficient condition (3.1)

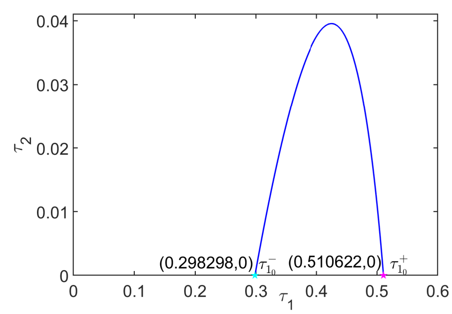

Figure 9. The stability switch curves on τ_1-τ_2 plane with $b = 0.25$.

Table 5. The Hopf bifurcation values of fixed $\tau_2 = 0$

ω	$\omega_+ \approx 1.517867$		$\omega_- \approx 1.213718$	
τ_1	$\tau_{1_0}^+ \approx 0.510622$	$\tau_{1_1}^+ \approx 4.650105$	$\tau_{1_0}^- \approx 0.298298$	$\tau_{1_1}^- \approx 5.475104$
$\mathrm{Re}(C_1(0))$	-0.081421	1.151347	-0.091441	1.011758
$\mathrm{Re}\{\lambda'(\tau_{1_0}^{\pm})\}$	0.878288	0.039121	-0.319594	-0.028766
μ_2	0.092704	-29.430151	-0.286116	35.171786
β_2	-0.162842	2.302693	-0.182882	2.023516

stable for $\mathrm{Re}\{\lambda'(\tau_{1_0}^-)\} < 0$ at $\tau_{1_0}^-$; when $\tau_1 = 0.55 > \tau_{1_0}^+$ and $\tau_2 = 0$, E_-^* of model (1.5) becomes unstable and there exists a periodic oscillation in model (1.5) bifurcating from equilibrium E_{-}^{*} for $\mathrm{Re}\{\lambda'(\tau_{1_0}^{+})\} > 0$ and $\mu_2 > 0$ at $\tau_{1_0}^{+}$(see Fig. 10).

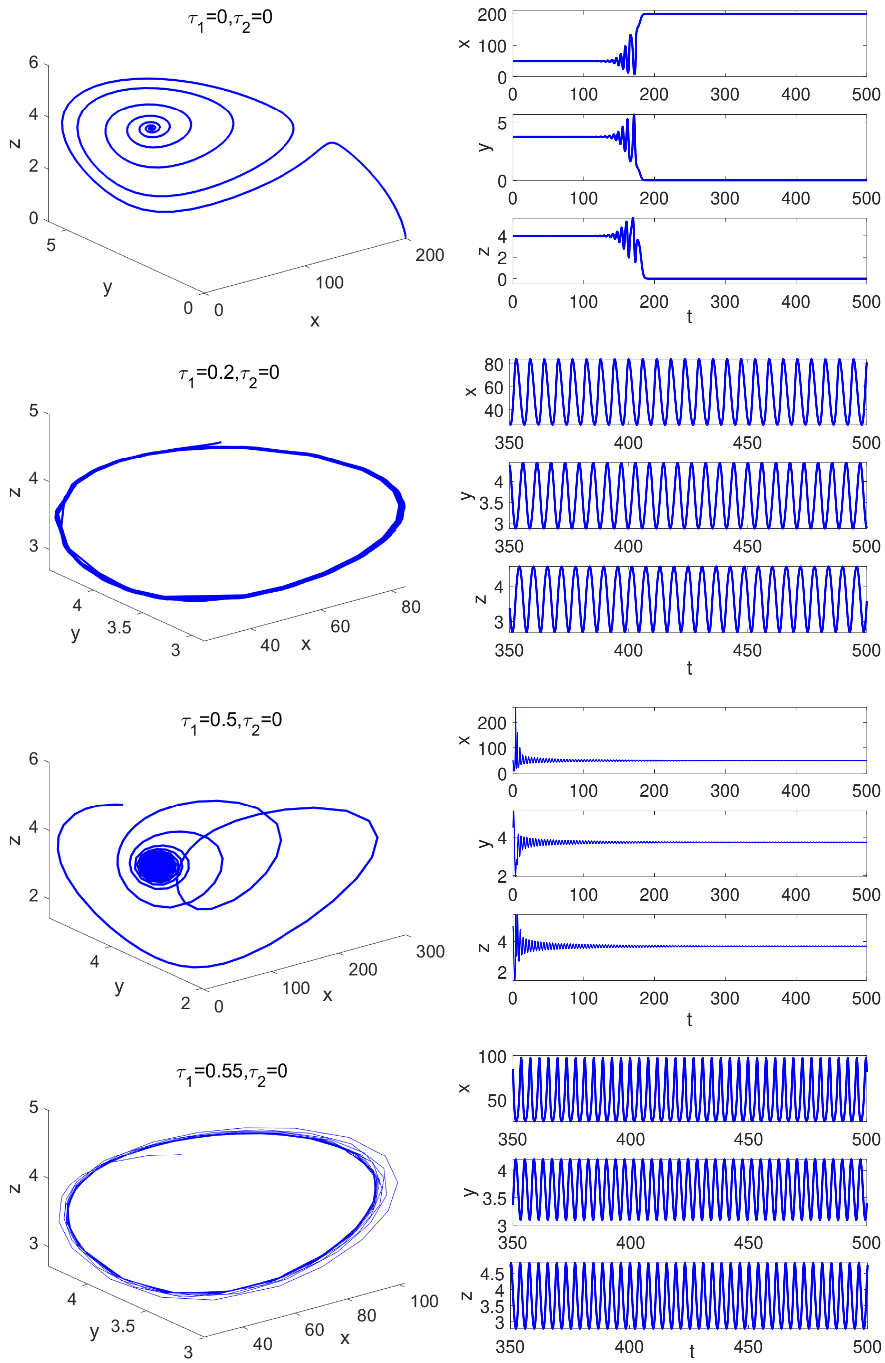

Figure 10. The phase plane and solution curves of model (1.5) with $b = 0.25$

If we choose different coefficients and different delays of model (1.5), then model (1.5) has different chaotic attractors (see Figs. 11 and 12).

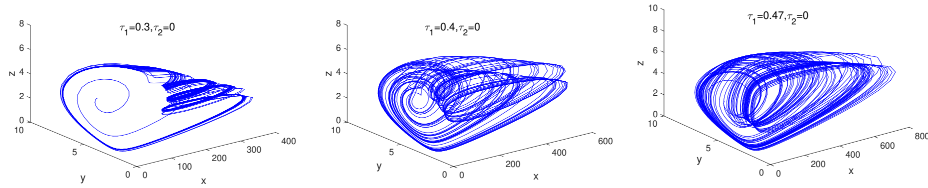

Figure 11. The phase diagrams of the chaos in model (1.5) with $K = 260$, $a = 0.02$, $b = 0.25$, $c = 1.2$, $r = 6.2$, $\beta = 1$, $\delta = 0.9$.

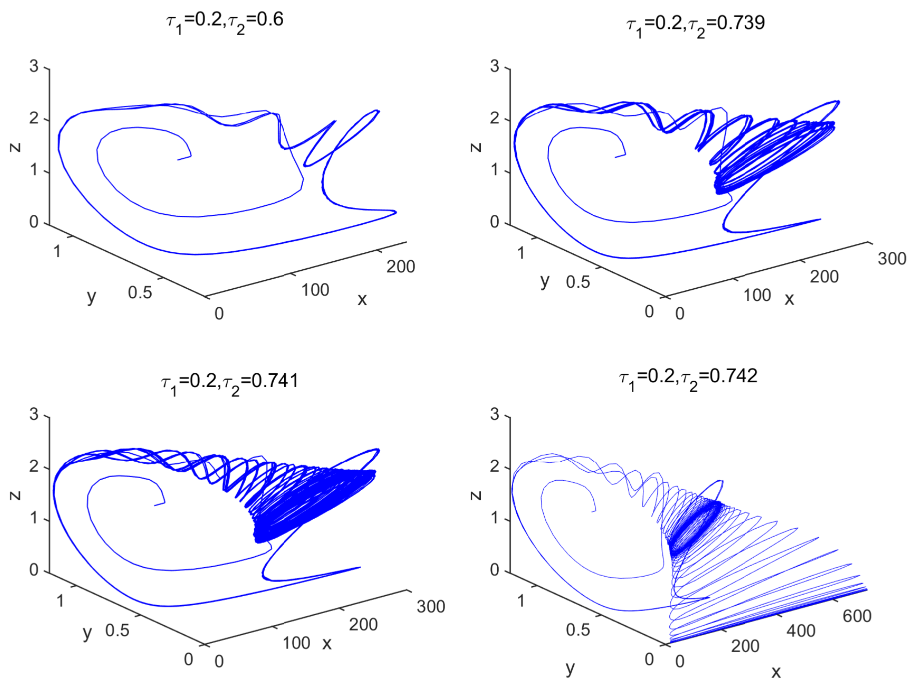

Figure 12. The phase diagrams of model (1.5) with $K = 250$, $a = 0.2$, $b = 0.6$, $c = 10$, $r = 10$, $\beta = 5$, $\delta = 1$.

4. Conclusion

Based on the model of combinational immune boost against tumor by Nagata and Furuta et al [14], we propose a combinational immune anti-tumor model with double delays, and investigate the effect of time delays on dynamical behaviors of model (1.5). By theoretical analysis, we find that there exist stability switches, and some steady coexistence, such as bi-stability states of two equilibria and the coexistence of two periodic solutions with different stabilities and different amplifications in model

(1.5). On the other hand, the stability conditions of equilibrium E_-^* reveal that both time delays and the activation rate of T cells are important factors for controlling tumor growth. Numerical simulations show rich dynamic behaviors around the double Hopf bifurcation points, including chaotic attractors and their corresponding Poincaré maps, as well as the progress transmission of unstable-oscillation-stable-oscillation. Therefore, doctors can develop some new drugs to destroy the tumor growth microenvironment to prolong the feedback time of tumor growth for controlling the tumor growth state. On the other hand, numerical simulations reveals that the existence of chaos in model (1.5) not only strongly depends on the initial values of tumor cells and T cells, but also is related to the occurrences of several Hopf bifurcations with the same time delays simultaneously. In addition, different coefficients and different delays of model (1.5) have different chaotic attractors.

Acknowledgments

This work is supported by the National Natural Science Foundation of China (No. 11801122).

Appendix

In this section, the detailed calculations of bifurcation properties are given by using the normal form theory and the center manifold theory [5]. Without loss of generality, we assume that $\tau_2^* > \tau_{1_0}^+$ and $\tau_1 \in [0, \tau_{1_0}^+)$. Rescaling the time by $t \longmapsto (t/\tau_2)$, let $\tilde{x}(t) = x(t) - x_-^*$, $\tilde{y}(t) = y(t) - y_-^*$, $\tilde{z}(t) = z(t) - z^*$ and still denote $\tilde{x}(t)$, $\tilde{y}(t)$, $\tilde{z}(t)$ by $x(t)$, $y(t)$, $z(t)$. We introduce a bifurcation parameter by $\tau_2 = \tau_2^* + \mu$ and expand the function, then model(1.5) can be transformed into an FDE in $\mathbb{C}^1([-1, 0], \mathbb{R}^3)$.

$$\dot{X}(t) = L_\mu(X_t) + F(\mu, X_t), \tag{4.1}$$

where $X_t(\theta) = X(t + \theta)$ and $L_\mu : \mathbb{C}^1([-1, 0], \mathbb{R}^3) \to \mathbb{R}^3$ is defined by

$$L_\mu(\varphi) = (\tau_2^* + \mu)\left[A\varphi(0) + B\varphi(-\frac{\tau_1}{\tau_2^* + \mu}) + C\varphi(-1)\right],$$

where $A = \begin{pmatrix} 0 & -cx_-^* & 0 \\ 0 & 0 & by_-^* \\ 0 & 0 & -\beta \end{pmatrix}$, $B = \begin{pmatrix} -\frac{rx_-^*}{K} & 0 & 0 \\ 0 & 0 & 0 \\ 0 & 0 & 0 \end{pmatrix}$, $C = \begin{pmatrix} 0 & 0 & 0 \\ 0 & 0 & 0 \\ ay_-^* & ax_-^* & 0 \end{pmatrix}$,

$$\varphi(t) = (\varphi_1(t), \varphi_2(t), \varphi_3(t))^{\mathrm{T}} \in \mathbb{C}^1([-1, 0], \mathbb{R}^3),$$

and

$$F(\mu, \varphi) = (\tau_2^* + \mu)\begin{pmatrix} -c\varphi_1(0)\varphi_2(0) - \frac{r}{K}\varphi_1(0)\varphi_1(-\frac{\tau_1}{\tau_2^*+\mu}) \\ b\varphi_2(0)\varphi_3(0) \\ a\varphi_1(-1)\varphi_2(-1) \end{pmatrix}.$$

By the Riesz representation theorem, there exists a function $\eta(\theta,\mu)$ of bounded variations for $\theta\in[-1,0]$ such that

$$L_\mu(\varphi)=\int_{-1}^{0}[d\eta(\theta,\mu)]\varphi(\theta) \tag{4.2}$$

for $\varphi\in\mathbb{C}^1([-1,0],\mathbb{R}^3)$. In fact, we can choose

$$\eta(\theta,\mu)=\begin{cases}0, & \theta=-1,\\ (\tau_2^*+\mu)C, & \theta\in(-1,-\dfrac{\tau_1}{\tau_2^*+\mu}),\\ (\tau_2^*+\mu)(B+C), & \theta\in[-\dfrac{\tau_1}{\tau_2^*+\mu},0),\\ (\tau_2^*+\mu)(A+B+C), & \theta=0.\end{cases}$$

Then Eq. (4.2) is satisfied.

For $\varphi\in\mathbb{C}^1([-1,0],\mathbb{R}^3)$, define the operator $\mathcal{A}(\mu)$ as

$$\mathcal{A}(\mu)\varphi(\theta)=\begin{cases}\dfrac{\mathrm{d}\varphi(\theta)}{\mathrm{d}\theta}, & \theta\in[-1,0),\\ \displaystyle\int_{-1}^{0}[\mathrm{d}\eta(\xi,\mu)]\varphi(\xi), & \theta=0.\end{cases} \tag{4.3}$$

and

$$\mathcal{R}(\mu)\varphi(\theta)=\begin{cases}0, & \theta\in[-1,0),\\ F(\mu,\varphi), & \theta=0.\end{cases} \tag{4.4}$$

Then system (4.1) is equivalent to the following operator equation

$$\dot{X}(t)=\mathcal{A}(\mu)X_t+\mathcal{R}(\mu)X_t \tag{4.5}$$

where $X_t=X(t+\theta)$ for $\theta\in[-1,0]$.

For $\psi\in\mathbb{C}^1([0,1],(\mathbb{R}^3)^*)$, define an operator

$$\mathcal{A}^*\psi(s)=\begin{cases}-\dfrac{\mathrm{d}\psi(s)}{\mathrm{d}s}, & s\in(0,1],\\ \displaystyle\int_{-1}^{0}\psi(-\xi)\mathrm{d}\eta(\xi,0), & s=0,\end{cases}$$

and a bilinear form

$$\langle\psi(s),\varphi(\theta)\rangle=\overline{\psi}(0)\varphi(0)-\int_{-1}^{0}\int_{\xi=0}^{\theta}\overline{\psi}(\xi-\theta)\mathrm{d}\eta(\theta)\varphi(\xi)\mathrm{d}\xi,$$

where $\eta(\theta)=\eta(\theta,0)$. Then $\mathcal{A}(0)$ and $\mathcal{A}^*$ are adjoint operators. From the discussion above, we know that $\pm i\omega_{\tau_1}^k\tau_2^*$ are eigenvalues of $\mathcal{A}(0)$ and therefore they are also eigenvalues of $\mathcal{A}^*$. We can verify that the vector $q(\theta)=(q_1,q_2,q_3)^{\mathrm{T}}e^{i\omega_{\tau_1}^k\tau_2^*\theta}$ ($\theta\in[-1,0]$) and $q^*(s)=\frac{1}{\bar{d}}(q_1^*,q_2^*,q_3^*)e^{i\omega_{\tau_1}^k\tau_2^*s}$ ($s\in[0,1]$) are the eigenvectors of $\mathcal{A}(0)$ and $\mathcal{A}^*$ corresponding to the eigenvalues $i\omega_{\tau_1}^k\tau_2^*$ and $-i\omega_{\tau_1}^k\tau_2^*$, respectively, where

$$(q_1,q_2,q_3)^{\mathrm{T}}=\left(\frac{-cKx_-^*}{i\omega_{\tau_1}^kK+rx_-^*e^{-i\omega_{\tau_1}^k\tau_1}},1,\frac{i\omega_{\tau_1}^k}{by_-^*}\right)^{\mathrm{T}},$$

$$(q_1^*, q_2^*, q_3^*) = \left(\frac{aKy_-^* e^{i\omega_{\tau_1}^k \tau_2^*}}{-i\omega_{\tau_1}^k K + rx_-^* e^{i\omega_{\tau_1}^k \tau_1}}, \frac{-i\omega_{\tau_1}^k + \beta}{by_-^*}, 1 \right),$$

$$d = q_1\overline{q}_1^* + q_2\overline{q}_2^* + q_3\overline{q}_3^* - \tau_1 q_1\overline{q}_1^* \frac{rx_-^*}{K} e^{-i\omega_{\tau_1}^k \tau_1} + \tau_2^*(q_1 y_-^* + q_2 x_-^*) a\overline{q}_3^* e^{-i\omega_{\tau_1}^k \tau_2^*}.$$

Moreover, $\langle q^*(s), q(\theta)\rangle = 1$, $\langle q^*(s), \overline{q}(\theta)\rangle = 0$.

Following are the algorithms given in [5] and using a computation process similar to that in [13, 25, 28], we obtain the coefficients used in determining the important quantities:

$$\begin{aligned}
g_{20} =& \frac{2\tau_2^*}{d}[\overline{q}_1^*(-cq_1q_2 - \frac{r}{K}q_1^2 e^{-i\omega_{\tau_1}^k \tau_1}) + \overline{q}_2^* b q_2 q_3 + \overline{q}_3^* a q_1 q_2 e^{-2i\omega_{\tau_1}^k \tau_2^*}],\\
g_{11} =& \frac{\tau_2^*}{d}[-c\overline{q}_1^*(q_1\overline{q}_2 + q_2\overline{q}_1) - \frac{r}{K}\overline{q}_1^* q_1\overline{q}_1(e^{i\omega_{\tau_1}^k \tau_1} + e^{-i\omega_{\tau_1}^k \tau_1}) + b\overline{q}_2^*(q_2\overline{q}_3 + q_3\overline{q}_2)\\
&+ a\overline{q}_3^*(q_1\overline{q}_2 + q_2\overline{q}_1)],\\
g_{02} =& \frac{2\tau_2^*}{d}[\overline{q}_1^*(-c\overline{q}_1\overline{q}_2 - \frac{r}{K}\overline{q}_1^2 e^{i\omega_{\tau_1}^k \tau_1}) + \overline{q}_2^* b\overline{q}_2\overline{q}_3 + \overline{q}_3^* a\overline{q}_1\overline{q}_2 e^{2i\omega_{\tau_1}^k \tau_2^*}],\\
g_{21} =& \frac{2\tau_2^*}{d}\{-c\overline{q}_1^*[q_1 W_{11}^{(2)}(0) + q_2 W_{11}^{(1)}(0) + \frac{1}{2}\overline{q}_1 W_{20}^{(2)}(0) + \frac{1}{2}\overline{q}_2 W_{20}^{(1)}(0)]\\
&- \frac{r}{K}\overline{q}_1^*[q_1(W_{11}^{(1)}(-\frac{\tau_1}{\tau_2^*}) + W_{11}^{(1)}(0)e^{-i\omega_{\tau_1}^k \tau_1}) + \frac{1}{2}\overline{q}_1(W_{20}^{(1)}(-\frac{\tau_1}{\tau_2^*}) + W_{20}^{(1)}(0)e^{i\omega_{\tau_1}^k \tau_1})]\\
&+ b\overline{q}_2^*[q_2 W_{11}^{(3)}(0) + q_3 W_{11}^{(2)}(0) + \frac{1}{2}\overline{q}_2 W_{20}^{(3)}(0) + \frac{1}{2}\overline{q}_3 W_{20}^{(2)}(0)]\\
&+ a\overline{q}_3^*[(q_1 W_{11}^{(2)}(-1) + q_2 W_{11}^{(1)}(-1))e^{-i\omega_{\tau_1}^k \tau_2^*}\\
&+ \frac{1}{2}(\overline{q}_1 W_{20}^{(2)}(-1) + \overline{q}_2 W_{20}^{(1)}(-1))e^{i\omega_{\tau_1}^k \tau_2^*}]\}.
\end{aligned}$$

where for $\theta \in [-1, 0]$, denoting $W_{20}(\theta) = (W_{20}^{(1)}(\theta), W_{20}^{(2)}(\theta), W_{20}^{(3)}(\theta))^{\mathrm{T}}$, and $W_{11}(\theta) = (W_{11}^{(1)}(\theta), W_{11}^{(2)}(\theta), W_{11}^{(3)}(\theta))^{\mathrm{T}}$. Through routine calculation, we have

$$\begin{aligned}
W_{20}(\theta) &= \frac{ig_{20}}{\omega_{\tau_1}^k \tau_2^*} q(0) e^{i\omega_{\tau_1}^k \tau_2^* \theta} + \frac{i\overline{g}_{02}}{3\omega_{\tau_1}^k \tau_2^*}\overline{q}(0) e^{-i\omega_{\tau_1}^k \tau_2^* \theta} + \varepsilon_1 e^{2i\omega_{\tau_1}^k \tau_2^* \theta},\\
W_{11}(\theta) &= \frac{-ig_{11}}{\omega_{\tau_1}^k \tau_2^*} q(0) e^{i\omega_{\tau_1}^k \tau_2^* \theta} + \frac{i\overline{g}_{11}}{\omega_{\tau_1}^k \tau_2^*}\overline{q}(0) e^{-i\omega_{\tau_1}^k \tau_2^* \theta} + \varepsilon_2,
\end{aligned}$$

where ε_1 and ε_2 are both three-dimensional vectors

$$\varepsilon_1 = T_1^{-1} \begin{pmatrix} 2(-cq_1q_2 - \frac{r}{K}q_1^2 e^{-i\omega_{\tau_1}^k \tau_1}) \\ 2bq_2q_3 \\ 2aq_1q_2 e^{-2i\omega_{\tau_1}^k \tau_2^*} \end{pmatrix},$$

$$\varepsilon_2 = T_2^{-1} \begin{pmatrix} -c(q_1\overline{q}_2 + q_2\overline{q}_1) - \frac{r}{K}q_1\overline{q}_1(e^{i\omega_{\tau_1}^k \tau_1} + e^{-i\omega_{\tau_1}^k \tau_1}) \\ b(q_2\overline{q}_3 + q_3\overline{q}_2) \\ a(q_1\overline{q}_2 + q_2\overline{q}_1) \end{pmatrix},$$

and

$$T_1 = \begin{pmatrix} 2i\omega_{\tau_1}^k + \frac{rx_-^*}{K}e^{-2i\omega_{\tau_1}^k \tau_1} & cx_-^* & 0 \\ 0 & 2i\omega_{\tau_1}^k & -by_-^* \\ -ay_-^* e^{-2i\omega_{\tau_1}^k \tau_2^*} & -ax_-^* e^{-2i\omega_{\tau_1}^k \tau_2^*} & 2i\omega_{\tau_1}^k + \beta \end{pmatrix},$$

$$T_2 = \begin{pmatrix} \frac{rx_-^*}{K} & cx_-^* & 0 \\ 0 & 0 & -by_-^* \\ -ay_-^* & -ax_-^* & \beta \end{pmatrix}.$$

Similarly, the Hopf bifurcation properties for τ_2 in its stable interval and regarding τ_1 as a parameter can be obtained.

References

[1] Q. An, E. Beretta, Y. Kuang, et al., *Geometric stability swith criteria in delay differential equations with two delays and delay dependent parameters*, J. Differ. Equ., 2019, 266(11), 7073–7100.

[2] P. Bi, S. Ruan and X. Zhang, *Periodic and chaotic oscillations in a tumor and immune system interaction model with three delays*, Chaos, 2014, 24(2), 023101.

[3] Y. Du, B. Niu and J. Wei, *Two delays induce Hopf bifurcation and double Hopf bifurcation in a diffusive Leslie-Gower predator-prey system*, Chaos, 2019, 29, 013101.

[4] J. Hale, *Theory of Functional Differential Equations*, Springer-Verlag, New York, 1977.

[5] B. D. Hassard, N. D. Kazarinoff and Y. Wan, *Theory and Applications of Hopf Bifurcation*, Cambridge University Press, Cambridge, 1981.

[6] Z. Jiang and Y. Guo, *Hopf bifurcation and stability crossing curve in a planktonic resource-consumer system with double delays*, Int. J. Bifurcation Chaos, 2020, 30(13), 2050190.

[7] V. A. Kuznetsov, I. A. Makalkin, M. A. Taylor, et al., *Nonlinear dynamics of immunogenic tumors: parameter estimation and global bifurcation analysis*, Bull. Math. Biol., 1994, 56(2), 295–321.

[8] D. Kirschner and J. C. Panetta, *Modeling immunotherapy of the tumor-immune interaction*, J. Math. Biol., 1998, 37, 235–252.

[9] X. Lai, A. Stiff, M. Duggan, et al., *Modeling combination therapy for breast cancer with bet and immune check inhibitors*, P. Natl. Acad. Sci. USA, 2018, 115(21), 5534–5539.

[10] Y. Liu and J. Wei, *Bifurcation analysis in delayed Nicholson blowflies equation with delayed harvest*, Nonlinear Dyn., 2021, 105, 1805–1819.

[11] X. Lin and H. Wang, *Stability analysis of delay differential equations with two discrete delays*, Canad. Appl. Math. Quart., 2012, 20(4), 519–533.

[12] M. Li and H. Shu, *Multiple stable periodic oscillations in a mathematical model of CTL response to HTLV-I infection*, Bull. Math. Biol., 2011, 73, 1774–1793.

[13] K. Li and J. Wei, *Stability and Hopf bifurcation analysis of a prey-predator system with two delays*, Chaos Soliton Fract., 2009, 42(5), 2606–2613.

[14] M. Nagata, Y. Furta, Y. Takeuchi, et al., *Dynamical behavior of combinational immune boost against tumor*, Jpn. J. Ind. Appl. Math., 2015, 32(3), 759–770.

[15] B. Niu, Y. Guo and Y. Du, *Hopf bifurcation induced by delay effect in diffusive tumor-immune system*, Int. J. Bifurcat Chaos, 2018, 28(11), 1850136.

[16] S. Ruan, *Nonlinear dynamics in tumor-immune system interaction models with delays*, Discrete Cont. Dyn. B., 2021, 26(1), 541–602.

[17] S. Ruan and J. Wei, *On the zeros of a third degree exponential polynomial with applications to a delayed model for the control of testosterone secretion*, IMA J. Math. Appl. Med. Biol., 2001, 18, 41–52.

[18] S. Ruan and J. Wei, *On the zeros of transcendental functions with applications to stability of delay differential equations with two delays*, Dyn. Contin. Discrete Impuls. Syst. Ser. A Math. Anal., 2003, 10, 863–874.

[19] A. Rescigno and C. Delisi, *Immune surveillance and neoplasia¡ªII A two-stage mathematical model*, Bull. Math. Biol., 1977, 39(4), 487–497.

[20] H. Song, W. Jiang and S. Liu, *Virus dynamics model with interacelluar delays and immune response*, Math. Biosci. Eng., 2015, 12(1), 1–24.

[21] Y. Shu, J. Huang, Y. Dong, et al., *Mathematical modeling and bifurcation analysis of pro-and anti-tumor macrophages*, Appl. Math. Model., 2020, 88, 758–773.

[22] H. Shu, W. Xu, X. Wang, et al., *Complex dynamics in a delay differential equation with two delays in tick growth with diapause*, J. Differ Equ., 2020, 269, 10937–10963.

[23] Z. Song and J. Xu, *Stability switches and double Hopf bifurcation in a two-neural network system with multiple delays*, Cogn. Neurodynamics, 2013, 7(6), 505–521.

[24] Y. Tian and Y. Yuan, *Effect of time delays in an HIV virotherapy model with nonlinear incidence*, Proc. R. Soc. A., 2016, 472, 20150626.

[25] J. Wang, H. Shi, L. Xu, et al., *Hopf bifurcation and chaos of tumor-Lymphatic model with two time delays*, Chaos Soliton Fract., 2022, 157, 111922.

[26] J. Wang and W. Jiang, *Hopf-zero bifurcation of a delayed predator-prey model with dormancy of predators*, J. Appl Anal Comput., 2017, 7(3), 1515–1069.

[27] J. Wang and S. Liu, *Turing and Hopf bifurcation in a diffusive tumor-immunemodel*, J. Nonlinear Moldeling Anal., 2021, 3(3), 477–493.

[28] J. Wang and W. Jiang, *Bifurcation and chaos of a delayed predator-prey model with dormancy of predators,* Nonlinear Dyn., 2012, 69, 1541–1558.

[29] Y. Yuan and J. Bélair, *Threshold dynamics in an SEIRS model with latency and temporary immunity*, J. Math. Biol., 2014, 69, 875–904.